

that of the keto form in the ground state measured by transient absorption (3.5  $\mu$ s).<sup>3,4</sup>

By using eq 1 with the experimental result ( $U_s/U_t = 0.105$ ) and the other parameters,  $E_{ex} = 29670$  cm<sup>-1</sup>,  $E_f^e = 26500$  cm<sup>-1</sup>,  $E_f^k = 18900$  cm<sup>-1</sup>,  $\phi_f^e = 0.044$ ,<sup>13</sup>  $\phi_f^k = 0.077$ ,<sup>13</sup> and  $\phi_t = 0.85$ ,<sup>4</sup>  $\Delta H$  is calculated to be 3400 cm<sup>-1</sup>. It is interesting to note that a quantum mechanically calculated  $\Delta H$  by Bordor et al. was 2000 cm<sup>-1</sup>,<sup>11</sup> relatively close to the experimental data.

(13) The quantum yields of fluorescence were determined relative to quinine sulfate in 0.5 M sulfuric acid as a standard solution.

From the spectroscopic data ( $E_f^e$ ,  $E_f^k$ ), and the obtained  $\Delta H$  in the ground state, the stabilization energy of the keto form in the excited ( $S_1$ ) state is calculated to be 4200 cm<sup>-1</sup> (Figure 1), much larger than the thermal energy at room temperature. The proton back-transfer rate in the excited state can therefore be negligibly small. This finding supports the kinetic model proposed by Itoh et al.<sup>4</sup>

In summary, we demonstrated that the time-resolved TL method is a very powerful method to measure the enthalpy difference of keto and enol forms in proton-transfer systems.

Registry No. 7-Hydroxyquinoline, 580-20-1.

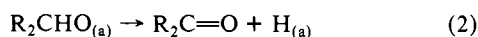
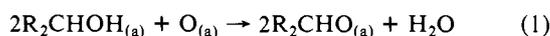
## Oxidation of *tert*-Butyl Alcohol to Isobutylene Oxide on a Ag(110) Surface: The Role of Unactivated C-H Bonds in Product Selectivity

Robert L. Brainard<sup>†</sup> and Robert J. Madix\*

Contribution from the Departments of Chemical Engineering and Chemistry, Stanford University, Stanford, California 94305. Received May 9, 1988

**Abstract:** *tert*-Butyl alcohol reacts with oxygen-covered Ag(110) surfaces below 200 K yielding *t*-BuO<sub>(a)</sub> and adsorbed water and hydroxyl groups. Temperature-programmed reaction spectroscopy demonstrates that *t*-BuO<sub>(a)</sub> reacts at 440 and 510 K by processes that involve rate-limiting C-H bond cleavage yielding isobutylene oxide, isobutylene, *tert*-butyl alcohol, H<sub>2</sub>O, and CO<sub>2</sub>. The reaction path at 440 K predominates when the initial coverage of O<sub>(a)</sub> is high; that at 510 K predominates when the coverage of O<sub>(a)</sub> is low. A third process occurs at 590 K, producing acetone. It is concluded from this work that the unactivated methyl C-H bonds in *t*-BuO<sub>(a)</sub> are significantly more stable toward cleavage by this surface than are the activated C-H bonds in MeO<sub>(a)</sub> or EtO<sub>(a)</sub>. Isotopic labeling experiments with <sup>18</sup>O<sub>2</sub> show that the surface oxygen present before the *tert*-butyl alcohol dose is not incorporated into the isobutylene oxide, acetone, or *tert*-butyl alcohol products. The reactions occurring at 440 and 510 K appear to involve rate-limiting C-H bond breaking reactions yet do not involve transfer of hydrogen atoms to the surface. Instead, direct proton transfer from the methyl group of *t*-BuO<sub>(a)</sub> to either O<sub>(a)</sub> (440 K) or another *t*-BuO<sub>(a)</sub> (510 K) appears to occur.

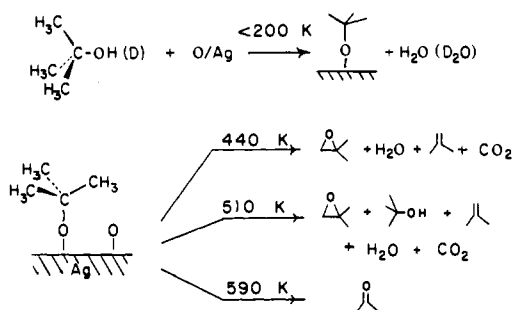
The oxidation of primary and secondary alcohols on Ag(110) and Cu(110) surfaces under ultrahigh vacuum conditions (UHV) is now fairly well understood.<sup>1-5</sup> Generally, the first step involves the reaction of an adsorbed alcohol molecule with surface oxygen to form a surface-bound alkoxide and water (eq 1; R = H, alkyl).



Upon further heating, the surface alkoxide reacts and yields an aldehyde (or ketone) and H<sub>(a)</sub>, presumably by reaction of the hydrogen  $\alpha$  to oxygen with the surface (eq 2). Recombination reactions produce the parent alcohol, water, and/or H<sub>2</sub> (eq 3-5). Displacement reactions between surface alkoxides produced as in eq 1 and other alcohols or other proton donors have been useful in establishing a scale of stabilities of the surface alkoxides that agrees with the relative gas-phase acidities of the respective alcohols.<sup>6,7</sup>

The activation energies of reactions occurring according to eq 2 correlate with the bond strength of the C-H bond  $\alpha$  to oxygen.<sup>5</sup> In general, these C-H bonds are weaker than "unactivated" C-H bonds by 4-7 kcal/mol due to their proximity to oxygen. An

Scheme I. Reaction of *tert*-Butyl Alcohol ( $d_0$ ,  $d_1$ ) on Preoxygenated Ag(110) Surface



\* Products of the reactions occurring at 440 and 510 K are listed in order of decreasing yield.

unactivated C-H bond is defined<sup>8</sup> as a C-H bond that is not  $\alpha$  to a heteroatom or an unsaturated center. The activated C-H bonds are weaker (have lower bond dissociation energies) because homolytic cleavage of these bonds produces carbon-centered radicals that are stabilized by the adjacent heteroatoms or unsaturated centers.

- (1) Wachs, I. E.; Madix, R. J. *Surf. Sci.* **1978**, *76*, 531-558.
- (2) Wachs, I. E.; Madix, R. J. *Appl. Surf. Sci.* **1978**, *1*, 303-328.
- (3) Wachs, I. E.; Madix, R. J. *J. Catal.* **1978**, *53*, 208-227.
- (4) Bowker, M.; Madix, R. J. *Surf. Sci.* **1980**, *95*, 190-206.
- (5) Bowker, M.; Madix, R. J. *Surf. Sci.* **1982**, *116*, 549-572.
- (6) Barteau, M. A.; Madix, R. J. *Surf. Sci.* **1982**, *115*, 355-381.
- (7) Barteau, M. A.; Madix, R. J. *Surf. Sci.* **1982**, *120*, 262-272.
- (8) Janowicz, A. H.; Bergman, R. G. *J. Am. Chem. Soc.* **1983**, *105*, 3929-3939.

<sup>†</sup> Current address: Polaroid Corp., 1265 Main Street, W4-2A, Waltham, MA 02254.

We report here the reaction of *tert*-butyl alcohol on preoxygenated Ag(110) surfaces as studied by temperature-programmed reaction spectroscopy (TPRS).<sup>9</sup> This is the first study of the reaction of a tertiary alcohol with a metal surface, although tertiary metal alkoxides are well-known as ligands in organometallic chemistry.<sup>10-12</sup> This alcohol lacks a hydrogen  $\alpha$  to oxygen and thus, generally, exhibits much different chemistry than do primary and secondary alcohols. In this study we find that *tert*-butyl alcohol reacts with oxygen adsorbed on Ag(110) below 200 K yielding *t*-BuO<sub>(a)</sub> and water, as do primary alcohols; however, on further heating *t*-BuO<sub>(a)</sub> reacts at significantly higher temperatures (420–600 K) by processes involving cleavage of the methyl C–H bonds yielding isobutylene oxide (major product), *tert*-butyl alcohol, water, isobutylene, acetone, CO, and CO<sub>2</sub> (Scheme I).

Two types of C–H bond breaking reactions are observed: one is assisted by surface oxygen, the other is not. In both cases, C–H bond cleavage is involved in the rate-limiting step. This study thus provides mechanistic details for a reaction that is fundamental to heterogeneous catalysis: the cleavage of an “unactivated” C–H bond by a metal surface. In addition, these reactions occur at temperatures  $\sim$ 200 K higher than do the reactions that break the “activated” C–H bonds in methanol<sup>1</sup> and ethanol,<sup>2</sup> consistent with the difference in C–H bond strengths.

The oxidation of *t*-BuOH on this surface yields appreciable quantities of isobutylene oxide. The mechanistic interpretations of this reaction presented here involve a surface oxametallacycle and a rearrangement that may have mechanistic implications for the epoxidation of ethylene.

## Experimental Section

**General Procedures.** Experiments were performed in a vacuum system consisting of a stainless steel bell jar, evacuated by an ion pump to a base pressure of  $2 \times 10^{-10}$  Torr. The chamber was equipped with a UTI 100 C mass spectrometer, LEED optics, an argon ion gun, and a double-pass CMA for Auger and XPS. The mass spectrometer was equipped with a glass collimator, which minimized spurious TPRS peaks due to the crystal support and was controlled by a multiplexer such that 8 masses could be monitored simultaneously. The mass spectrometer could also be controlled by a computer program that monitored up to 200 masses simultaneously. This program was used to check for unexpected products, especially those with high molecular weights. After such a survey of masses, however, all TPRS results presented here were determined by monitoring 2–8 masses in order to achieve higher temperature resolution of the product evolution curves. Coverage of O<sub>(a)</sub> was determined by calibrating integrals of O<sub>2</sub> desorption (600 K) at 0.25 and 0.33 ML<sup>13</sup> coverages determined by  $p(4 \times 1)$  and  $p(3 \times 1)$  LEED patterns.<sup>14</sup>

**Temperature-Programmed Reaction Spectroscopy (TPRS).** In a typical experiment, the clean Ag(110) crystal was dosed directly with 825 langmuirs of oxygen at 300 or 120 K<sup>15</sup> and then with *tert*-butyl alcohol from a separate dosing line. The single crystal was then positioned in front of the mass spectrometer and radiatively heated by a tungsten filament to 700 K. A linear heating rate of 10 K/s was used unless stated otherwise.

The reaction products were identified by comparing the transient mass spectra obtained with mass spectral data obtained from the pure reference compounds determined with the same spectrometer. The spectra of the reference samples were determined by two methods: (i) the sample was leaked into the chamber, and a background mass spectrum was

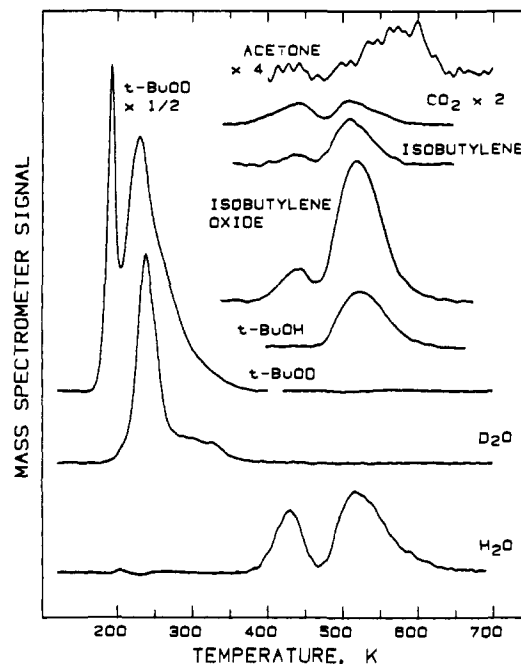


Figure 1. TPRS spectrum of the reaction of *tert*-butyl alcohol-*d*<sub>1</sub> (2.8 langmuirs, 120 K dose temperature) with a Ag(110) surface covered with 0.25 monolayer O<sub>(a)</sub>; 10 K/s heating rate.

taken, or (ii) the compound was condensed onto the clean Ag(110) crystal at 120 K and thermally desorbed into the mass spectrometer between 180 and 200 K. Both methods gave comparable results ( $\pm 10\%$ ). The identities of isobutylene oxide, isobutylene, *tert*-butyl alcohol, and acetone were determined by using 8–10 masses; the identities of CO<sub>2</sub>, H<sub>2</sub>O, H<sub>2</sub>, and D<sub>2</sub>O were determined by using 1–3 masses. In practice, however, one mass (*m/q*) was used to monitor each compound; namely, isobutylene oxide (42), *tert*-butyl alcohol (59), isobutylene (56), acetone (58). TPRS spectra were decomposed by a procedure described elsewhere.<sup>15</sup>

**Sample Preparation.** *tert*-Butyl alcohol-*d*<sub>0</sub> was recrystallized (neat) three times and distilled from C<sub>2</sub>H<sub>2</sub>. *tert*-Butyl alcohol-*d*<sub>0</sub> (ICN) was vacuum transferred twice, the first time from C<sub>2</sub>H<sub>2</sub>. Acetone was distilled twice under vacuum from K<sub>2</sub>CO<sub>3</sub>. Isobutylene oxide (Farchan Labs.) was pure by <sup>1</sup>H NMR and GC/MS and was used as received. *t*-BuOD (Aldrich) and isobutylene were also used as received.

The silver crystal was cleaned by argon bombardment at 8 mA for 20 min and annealed at 750 K for 4 min. Several cycles of oxygen doses and heating were used to clean small amounts of carbon from the surface. The cleanliness of this sample was verified by Auger spectroscopy and by observing the relative sizes of the O<sub>2</sub>, CO<sub>2</sub>, and H<sub>2</sub>O TPRS desorption peaks following an oxygen dose of 600 langmuirs. We considered surfaces that gave product ratios (O<sub>2</sub>/CO<sub>2</sub> and O<sub>2</sub>/H<sub>2</sub>O) subsequent to an oxygen exposure of greater than 20:1 to be clean. The Ag(110) crystal gave sharp LEED patterns characteristic of the (110) surface.

## Results

**Products (*t*-BuOD).** The products of the reaction of *t*-BuOD with the oxygen covered Ag(110) surface as determined by TPRS are shown in Figure 1. The surface of the Ag(110) crystal at 120 K covered with 0.25 ML of O<sub>(a)</sub> was dosed directly<sup>16</sup> with 2 langmuirs of *tert*-butyl alcohol-*d*<sub>1</sub> ((CH<sub>3</sub>)<sub>3</sub>CO*D*) and heated to 700 K. *tert*-Butyl alcohol-*d*<sub>1</sub> desorbs without reaction from a multilayer at 190 K and a molecularly bound state of submonolayer coverages at 230 K. D<sub>2</sub>O is evolved at distinct temperatures between 200 and 350 K characteristic of desorption of molecular water and disproportionation of OD groups on oxygen-predosed Ag(110);<sup>3,14,17</sup> clearly D<sub>2</sub>O is a product of a reaction in which the O–D bond of the alcohol is broken below 200 K. This result is a clear indication of the formation of *t*-BuO<sub>(a)</sub> according to eq 1. Water and CO<sub>2</sub>, as well as products having stoichiometry

(9) Portions of this work have been published previously. Brainard, R. L.; Madix, R. J. *J. Am. Chem. Soc.* **1987**, *109*, 8082–8083.

(10) Schrock, R. R. *J. Organomet. Chem.* **1986**, *300*, 249–262. Weinrovius, J. H.; Schrock, R. R. *Organometallics* **1982**, *1*, 148. Listemann, M. L.; Schrock, R. R. *Ibid.* **1985**, *4*, 74. Schrock, R. R.; Listemann, M. L.; Sturgeoff, L. G. *J. Am. Chem. Soc.* **1982**, *104*, 4291.

(11) Chisholm, M. H.; Hoffman, D. M.; Huffman, J. C. *Organometallics* **1985**, *4*, 986–993. Chisholm, M. H.; Reichert, W. W.; Cotton, F. A.; Murillo, C. A. *J. Am. Chem. Soc.* **1977**, *99*, 1652–1654. Rees, W. M.; Churchill, M. R.; Fettingtinger, J. C.; Atwood, J. D. *Organometallics* **1985**, *4*, 217–21859. Mehrotra, R. C. *J. Indian Chem. Soc.* **1982**, *59*, 715–722.

(12) Bradly, D. C.; Mehrotra, R. C.; Gaur, D. P. *Metal Alkoxides*; Academic Press: New York, 1978; pp 27–28.

(13) The monolayer (ML) is defined as the ratio of adsorbate molecules to surface metal atoms. One langmuir is defined as a dose of 10<sup>6</sup> Torr-s.

(14) Barteau, M. A.; Madix, R. J. In *The Chemical Physics of Solid Surfaces and Heterogeneous Catalysis*; King, D. A., Woodruff, D. P., Eds.; Elsevier Scientific: New York, 1982; Vol. 4, pp 94–142.

(15) Brainard, R. L.; Peterson, C. G.; Madix, R. J. *J. Am. Chem. Soc.*, in press.

(16) The enhancement factor for *tert*-butyl alcohol in these experiments was 140.

(17) Jorgenson, S. W.; Sauli, A. G.; Madix, R. J. *Langmuir* **1985**, *1*, 526–528.

corresponding to isobutylene oxide and isobutylene, are evolved in reaction-limited peaks at 440 and 510 K, while *tert*-butyl alcohol is formed only at 510 K. The formation of different product species at the same temperature indicates that their formation is dictated by the same rate-limiting step. Further, the observation that only *tert*-butyl alcohol- $d_0$  and  $H_2O$  form at these temperatures and the absence of *tert*-butyl alcohol- $d_1$  and  $D_2O$  or any deuterium-containing products shows that a methyl C-H bond in  $t\text{-BuO}_{(a)}$  is broken during each of these two steps at 440 and 510 K, respectively, since any deuterium released at these temperatures would certainly react immediately to form  $D_2$ ,  $D_2O$ , or  $t\text{-BuOD}$ ; none of which were formed.

A small amount of acetone is produced at 590 K.<sup>18</sup> Subsequent oxygen cleaning reactions indicate that a small amount of carbon also remains on the surface after the reaction. No reaction products were observed for the reaction of *tert*-butyl alcohol with the clean surface and no  $H_2$ ,  $CO$ ,  $CH_2O$ , and 2-butanone were produced under any conditions.<sup>19</sup>

The identity of the isobutylene and isobutylene oxide products was determined by mass spectrometry and by patterns of reactivity well established in organic chemistry. The ion fragmentation patterns observed for the desorbing alkene and the oxide were consistent with those published for isobutylene and isobutylene oxide.<sup>20</sup> They also agreed well with the fragmentation patterns we measured in the apparatus employed for these studies. This, in itself is insufficient proof of product identity, since different isomers often yield nearly identical cracking patterns at the electron energies used in our mass spectrometer.

For example, 1- and 2-butene and isobutylene give identical mass spectral cracking patterns. Furthermore, other species, such as tetrahydrofuran, give ratios of  $m/q$  42 and 72, which are very similar to the ratio observed for isobutylene oxide. The formation of such products, however, requires rearrangement of the carbon skeleton. It is clear that the formation of isobutylene and isobutylene oxide from  $t\text{-BuO}_{(a)}$  requires the least number of bonds to be formed or broken of the possible isomers, since the hydrocarbon skeleton remains intact. Formation of 1- or 2-butenes or of other oxidized products requires at the very least that a methyl group migrate. In the case of dihydrofuran, a ring closure must also occur. For reasons discussed below, we reject products involving alkyl migration and identify the products observed mass spectrometrically as isobutylene and isobutylene oxide.

**Variation in *tert*-Butyl Alcohol Dose.** The amount of *tert*-butyl alcohol dosed onto  $Ag(110)$  surfaces covered with 0.25 ML of oxygen was varied from 0.08 to 40 langmuirs in order to study the effect of the relative quantities of  $t\text{-BuO}_{(a)}$  and  $O_{(a)}$  present before the reaction. Since *tert*-butyl alcohol reacts with  $O_{(a)}$  during doses at room temperature to form  $t\text{-BuO}_{(a)}$  and water, large doses of *tert*-butyl alcohol both increase the coverage of  $t\text{-BuO}_{(a)}$  and decrease the coverage of  $O_{(a)}$  present following adsorption. Figure 2 shows the TPRS curves of isobutylene oxide, isobutylene, acetone, *tert*-butyl alcohol, and water over this range of *tert*-butyl alcohol doses. Low doses of *tert*-butyl alcohol favor the formation of isobutylene oxide near 440 K; large doses favor the formation near 510 K. More water is produced at 440 K than at 510 K, whereas *tert*-butyl alcohol is produced nearly exclusively at 510 K. These results indicate that  $t\text{-BuO}_{(a)}$  and/or some product of its decomposition reacts with  $O_{(a)}$  via the low-temperature route until the coverage of  $O_{(a)}$  is depleted; then  $t\text{-BuO}_{(a)}$  reacts in the absence of  $O_{(a)}$  via the high-temperature reaction route. This conclusion was verified by predosing with  $^{18}O_2$  (see below). Clearly,  $t\text{-BuO}_{(a)}$  is kinetically destabilized by excess oxygen, as observed for formate<sup>21</sup> and acetate<sup>22</sup> on the same surface.

(18) The acetone TPRS peak in Figure 1 is noisy due to the low gain settings employed to prevent the low-temperature multilayer and monolayer peaks of *tert*-butyl alcohol from being clipped.

(19) Small peaks for  $m/q = 2$  and 28 were observed in the nondeconvoluted spectra, but were completely accounted for by the cracking fractions of the other products (Table II).

(20) *Eight Peak Index of Mass Spectra*, 3rd ed.; The Mass Spectrometry Data Centre, Royal Society of Chemistry, The University, Nottingham, U.K., 1983.

(21) Sault, A. G.; Madix, R. J. *Surf. Sci.* **1986**, *176*, 415–424.

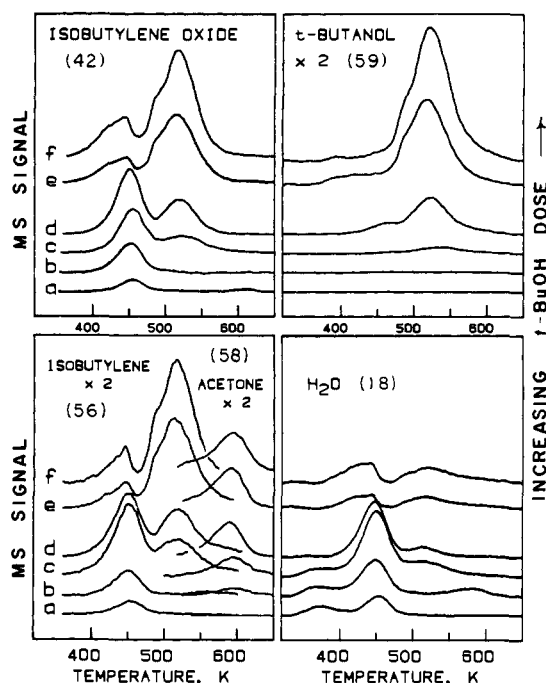
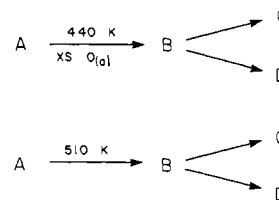


**Figure 2.** TPRS spectra resulting from variation of *tert*-butyl alcohol dose onto a  $Ag(110)$  surface at 300 K covered with 0.25 ML  $O_{(a)}$ ; 10 K/s heating rate; *tert*-butyl alcohol dose in langmuir (1 langmuir =  $10^{-6}$  Torr-s): (a) 0.08, (b) 0.2, (c) 0.4, (d) 1.0, (e) 4, (f) 40. The principle masses used to monitor each compound are listed in the figure.

#### Scheme II. Schematic Analysis of TPRS Data



The product yields relative to isobutylene oxide at a low ( $L = 0.08$  langmuir) and at a high *tert*-butyl alcohol dose ( $H = 40$  langmuirs) denoted as ( $L, H$ ) were, respectively, as follows: isobutylene oxide (100, 100), isobutylene (55, 55), *tert*-butyl alcohol (3, 50), acetone (5, 13), water (100, 26).

The TPRS peak shapes of the isobutylene oxide and isobutylene peaks provide two types of mechanistic information. First, the identical peak temperatures of these products in the two reaction channels specify that the rate of formation of these products is controlled by a single rate-limiting step for each channel, as the kinetic parameters for their formation are identical. That is, a single rate-limiting step controls the rate of formation of both isobutylene and isobutylene oxide at 440 K ( $A$  to  $B$  at 440 K, Scheme II) and a second rate-limiting step controls the rate of formation of isobutylene and isobutylene oxide at 510 K ( $A$  to  $B$  at 510 K, Scheme II). Second, the observation that the same relative amounts of isobutylene oxide and isobutylene (1.8:1) are produced in both reactions (at 440 and 510 K) suggests that both products are formed from the decomposition of a single intermediate common to *both* reaction channels (compound  $B$ , Scheme II).

**Variation in Oxygen Coverage.** Large quantities of *tert*-butyl alcohol (15 langmuirs) were dosed onto a  $Ag(110)$  surface at 300 K covered with 0.00–0.22 ML of  $O_{(a)}$  to study the effect of varying the coverage of  $t\text{-BuO}_{(a)}$  in the absence of  $O_{(a)}$ . When the coverage of oxygen is low and the room temperature dose of *tert*-butyl alcohol is high, all of the  $O_{(a)}$  reacts to form  $t\text{-BuO}_{(a)}$ . Unreacted *tert*-butyl alcohol does not stick. Figure 3 shows the isobutylene

(22) Sault, A. G.; Madix, R. J. *Surf. Sci.* **1986**, *172*, 598–614.

Table I. Arrhenius Activation Parameters and Kinetic Isotope Effects<sup>a</sup>

reactn	H or D <sup>b</sup>	E <sub>a</sub> , kcal/mol	log A <sup>c</sup>		k <sub>H</sub> /k <sub>D</sub> at	
			s <sup>-1</sup>	cm <sup>2</sup> /s	500 K <sup>d</sup>	300 K <sup>d</sup>
low temp	H	20 ± 1.5	9.4 ± 1	-4.9 ± 1	3.6 ± 1	7 ± 3
<i>t</i> -BuO <sub>(a)</sub> + O <sub>(a)</sub>	D	21 ± 1.5	9.3 ± 1	-5.0 ± 1		
high temp	H	17.2 ± 1	6.4 ± 0.6	-7.4 ± 1	1.6 ± 0.4	5 ± 2
<i>t</i> -BuO <sub>(a)</sub>	D	19 ± 1	7 ± 1	-6.9 ± 1		
acetone	H	23 ± 1	8 ± 0.7	-5.7 ± 1	1.0 ± 0.3	1.1 ± 0.4
product	D	23 ± 1	8 ± 1	-5.4 ± 1		

<sup>a</sup>The peak temperatures of several TPRS spectra of isobutylene oxide-*d*<sub>0</sub> (*m/q* = 42) and isobutylene oxide-*d*<sub>8</sub> (*m/q* = 46) at varied heating rates were used to determine the activation parameters for the low-temperature and high-temperature reactions. The peak temperatures of acetone-*d*<sub>0</sub> (*m/q* = 58) and acetone-*d*<sub>6</sub> (*m/q* = 18) were used to determine the activation parameters for acetone production. Only the acetone-*d*<sub>6</sub> spectra were decomposed to get its peak temperature. <sup>b</sup>Data for the reaction of *tert*-butyl alcohol-*d*<sub>9</sub> (D). <sup>c</sup>Since preexponential factors are helpful in determining the molecularity of a reaction (unimolecular vs bimolecular), it is necessary to examine these values in both unimolecular (s<sup>-1</sup>) and bimolecular (cm<sup>2</sup>/s) units. Unimolecular values were calculated directly from the data. An apparent first-order frequency factor is readily calculated. To obtain the order of magnitude of the second-order frequency factor the first-order value was divided by the surface concentration of the reactive intermediate, *t*-BuO<sub>(a)</sub>, at *T*<sub>p</sub>. <sup>d</sup>Kinetic isotope effects were determined by extrapolating to 500 and 300 K with Arrhenius activation parameters.

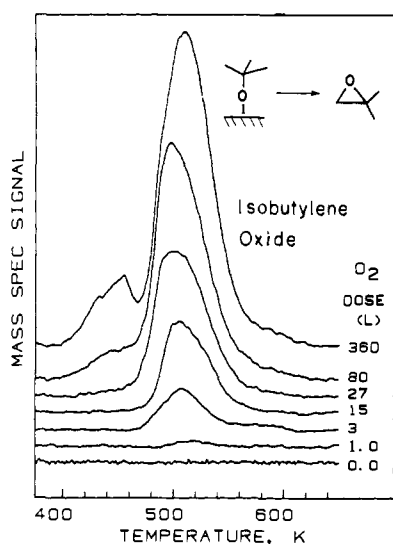


Figure 3. TPRS spectra of isobutylene oxide (*m/q* = 42, nondeconvoluted) as it desorbs following a dose of *tert*-butyl alcohol (15 langmuirs) onto a Ag(110) surface pre-dosed with variable quantities of oxygen (0.0–360 langmuirs). A heating rate of 8 K/s was used.

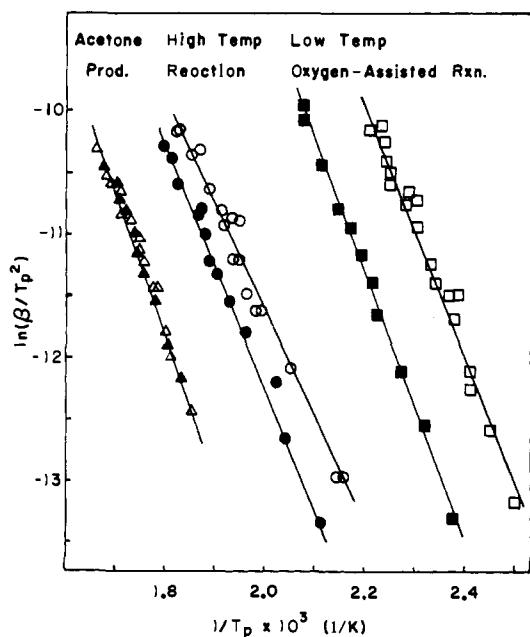


Figure 4. Arrhenius activation plots for the reaction of *tert*-butyl alcohol-*d*<sub>0</sub> (open figures) and *tert*-butyl alcohol-*d*<sub>9</sub> (solid figures) with pre-oxidized Ag(110) surfaces (0.25 ML of O<sub>(a)</sub>): low-temperature (oxygen-assisted) reaction (□, ■), high-temperature (oxygen-free) reaction (○, ●), and acetone-producing reaction (△, ▲).

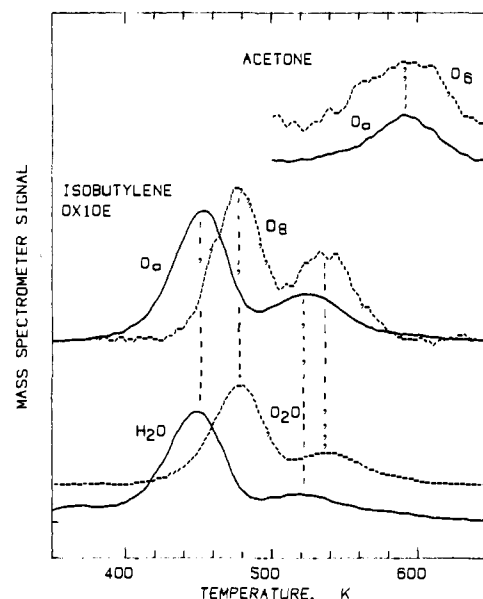
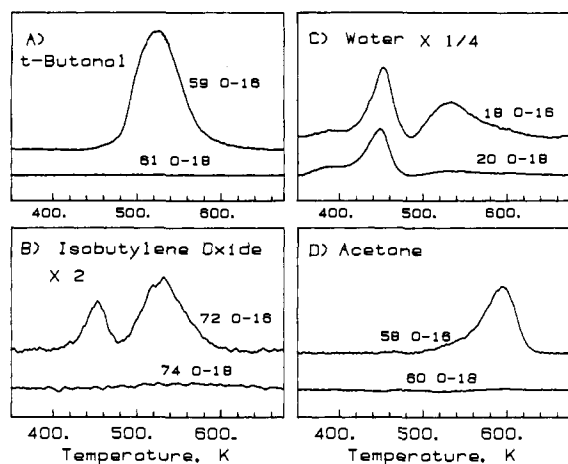


Figure 5. TPRS spectra (dashed) of isobutylene oxide-*d*<sub>8</sub>, D<sub>2</sub>O, and acetone-*d*<sub>6</sub> as they desorb following the reaction of *tert*-butyl alcohol-*d*<sub>9</sub> with O/Ag(110). TPRS spectra (solid) of isobutylene-*d*<sub>0</sub>, H<sub>2</sub>O, and acetone-*d*<sub>9</sub> following the reaction of *tert*-butyl alcohol-*d*<sub>0</sub> with O/Ag(110). The shift of the peaks to higher temperatures for the deuterated species is indicative of the kinetic isotope effect.

oxide peaks produced during these reactions. At low coverages of O<sub>(a)</sub> (0.002–0.11 ML), only the high-temperature peak (498–517 K) was observed. Higher oxygen exposures produced a small low-temperature peak (~425 K). There is a slight decrease in peak temperature with increasing coverages of *t*-BuO<sub>(a)</sub>.

**Arrhenius Activation Parameters.** Figure 4 shows Arrhenius plots for the low-temperature (440 K), high-temperature (510 K), and acetone-producing reactions (590 K) as determined by the method of heating-rate variation.<sup>23</sup> In a typical reaction, 1.0 langmuir of *tert*-butyl alcohol-*d*<sub>0</sub> or *tert*-butyl alcohol-*d*<sub>9</sub> ((C-D<sub>3</sub>)<sub>3</sub>COH) was dosed onto a Ag(110) surface covered with 0.25 ML O<sub>(a)</sub>. The heating rate was varied between 0.3 and 13 K/s. ln(β/*T*<sub>p</sub><sup>2</sup>) was plotted vs 1/*T*<sub>p</sub> for the six reactions (*d*<sub>0</sub> and *d*<sub>9</sub>). The values of the Arrhenius parameters obtained are listed in Table I.

**Kinetic Isotope Effects.** A TPRS experiment in which *tert*-butyl alcohol-*d*<sub>9</sub> ((CD<sub>3</sub>)<sub>3</sub>COH, 0.2 langmuir) was dosed onto a Ag(110) surface with an oxygen coverage of 0.25 ML produced TPRS peaks in which isobutylene oxide-*d*<sub>8</sub>, isobutylene-*d*<sub>8</sub>, *tert*-butyl alcohol-*d*<sub>10</sub>, and D<sub>2</sub>O desorbed at 475 and 535 K (Figure 5). Acetone-*d*<sub>6</sub> desorbed at 590 K. The kinetic isotope effects for the three reactions of interest were determined by interpolating (500 K) and extrapolating (300 K) from the Arrhenius activation data



**Figure 6.** Oxygen-18 labeling experiments. (A) *tert*-Butyl alcohol ( $^{16}\text{O}$ , 59 vs  $^{18}\text{O}$ , 61); (B) isobutylene oxide ( $^{16}\text{O}$ , 72 vs  $^{18}\text{O}$ , 74); (C)  $\text{H}_2\text{O}$  vs  $\text{H}_2^{18}\text{O}$ ; (D) acetone ( $^{16}\text{O}$ , 58 vs  $^{18}\text{O}$ , 60).

(Table I). Figure 5 clearly shows the kinetic isotope effect. The Arrhenius parameters could not be determined with sufficient accuracy to allow a significant comparison of either  $A_{\text{H}}$  and  $A_{\text{D}}$  or the differences in activation energy.

The low-temperature (oxygen-assisted) reaction has a large kinetic isotope effect ( $k_{\text{H}}/k_{\text{D}} = 3.6$  (500 K), 7 (300 K)). A kinetic isotope effect of 7 at 300 K is normally accepted to represent a reaction in which a C–H(D) bond is completely broken in the rate-limiting transition state.<sup>24</sup> Similarly, the high-temperature reaction shows a large kinetic isotope effect ( $k_{\text{H}}/k_{\text{D}} = 1.6$  (500 K), 5 (300 K)) and probably involves rate-limiting C–H(D) bond breaking. The reaction that produces acetone does not have a significant kinetic isotope effect and, thus, probably does not involve rate-limiting C–H(D) bond breaking.

**Oxygen-18 Labeling Experiments.** Experiments with  $^{18}\text{O}_2$  dosed on the surface were performed to distinguish the fates of the oxygen on the surface and that in the *tert*-butyl alcohol. *tert*-Butyl alcohol (0.4 langmuir) was dosed onto a Ag(110) surface covered with 0.1 ML  $^{18}\text{O}_{(\text{a})}$ . The resulting TPRS experiments showed that no  $^{18}\text{O}$  was incorporated into the *tert*-butyl alcohol, isobutylene oxide, or acetone (Figure 6). The masses ( $m/q$ ) used to follow the labeled and unlabeled products were as follows: *tert*-butyl alcohol (61, 59), isobutylene oxide (74, 72), and acetone (60, 58). The mass fragment used to monitor *tert*-butyl alcohol ( $m/q$  59) is the parent minus the methyl group and should contain oxygen. The masses used for isobutylene oxide and acetone are the parent masses and should also contain oxygen.<sup>25</sup> Both  $\text{H}_2\text{O}$  and  $\text{H}_2^{18}\text{O}$  are formed during this TPRS experiment. The low-temperature (oxygen-assisted) reaction produces approximately equal amounts of the two isotopes of water. The  $^{16}\text{O}_{(\text{a})}$  probably arises from decomposition of *t*-BuO $_{(\text{a})}$  yielding isobutylene. The high-temperature reaction, however, produces almost exclusively unlabeled water, suggesting that the low-temperature reaction cleans off all the  $^{18}\text{O}_{(\text{a})}$  and only the oxygen originating from *t*-BuO $_{(\text{a})}$  and isobutylene formation is available for reaction above 500 K.

**Secondary Oxidation Reactions of Isobutylene and Isobutylene Oxide.** The possibility of secondary reactions of isobutylene and isobutylene oxide was determined by studies of their reactions on the clean and oxygen-dosed Ag(110) surface. Isobutylene was dosed (2 langmuirs) onto a Ag(110) surface covered with 0.17 ML  $\text{O}_{(\text{a})}$ ; it reacts with oxidized silver surfaces and yields water,  $\text{CO}_2$ , and desorbs isobutylene (Figure 7A). No isobutylene oxide, *tert*-butyl alcohol, or acetone is produced. The absence of iso-

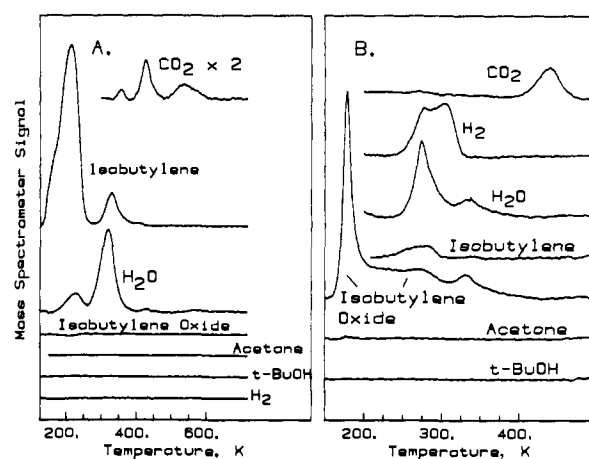


**Figure 7.** (A) TPRS spectra resulting from heating a Ag(110) surface covered with 0.17 ML  $\text{O}_{(\text{a})}$  and dosed with 2 langmuirs of isobutylene. (B) TPRS spectra resulting from heating a Ag(110) surface covered with 0.25 ML  $\text{O}_{(\text{a})}$  and dosed with 1 langmuir of isobutylene oxide.

butylene oxide as a product of the reaction between isobutylene and  $\text{O}_{(\text{a})}$  suggests that oxidation of isobutylene is not a viable reaction pathway for formation of isobutylene oxide from *t*-BuO $_{(\text{a})}$ .

Isobutylene oxide (3 langmuirs) was dosed onto a Ag(110) surface at 133 K covered with 0.25 ML  $\text{O}_{(\text{a})}$ . TPRS (Figure 7B) shows that isobutylene oxide reacts with the oxidized silver surface and yields  $\text{CO}_2$ , isobutylene, and  $\text{H}_2$ . No *tert*-butyl alcohol or acetone is produced. The observations that large amounts of  $\text{H}_2$  are produced and the observation that  $\text{CO}_2$  desorbs at a different temperature from that of the other products indicate that this reaction is fundamentally different from the reaction of *t*-BuO $_{(\text{a})}$  on these surfaces. Despite these complications, the observation that both isobutylene and isobutylene oxide react on these surfaces to form  $\text{CO}_2$  suggests that the production of  $\text{CO}_2$  from the decomposition of *t*-BuO $_{(\text{a})}$  may result from secondary oxidation of these products.

## Discussion

**Reaction Kinetics.** The peak shift observed for isobutylene oxide formation with *t*-BuO $_{(\text{a})}$  coverage is intermediate between that expected for a second-order reaction and that expected for a first-order reaction (Figure 3). Peak temperatures decreased by 20 K as the coverage of *t*-BuO $_{(\text{a})}$  increased from approximately 0.004 to 0.22 ML. At the highest oxygen exposures the peak temperature increased slightly. A bimolecular reaction occurring with Arrhenius activation parameters determined for this reaction (vide infra) should show a decrease in peak temperature of 60 K over this range of coverage. A true unimolecular reaction should not show any shift with coverage. This shift may be the result of through-space or through-surface repulsive lateral interactions.

The peak asymmetry also indicates that simple kinetics do not apply. The reaction that produces isobutylene also produces  $\text{O}_{(\text{a})}$ . Thus, although the high-temperature reaction begins when no  $\text{O}_{(\text{a})}$  is present,  $\text{O}_{(\text{a})}$  is generated during the course of the reaction along with isobutylene. Since the low-temperature oxygen-assisted reaction of *t*-BuO $_{(\text{a})}$  should be very fast at these temperatures, *t*-BuO $_{(\text{a})}$  should react by both of these pathways during the high-temperature TPRS peak. We attribute the asymmetric peak shapes and the unusual behavior of their peak shifts to these complex kinetics.

Preexponential factors can be very useful in determining the molecularity of reactions.<sup>26–28</sup> First-order reactions on surfaces typically have preexponential factors of  $10^{12}$ – $10^{16}$   $\text{s}^{-1}$ .<sup>29–32</sup> Bi-

(24) Melander, L.; Saunders, W. H. *Reaction Rates of Isotopic Molecules*; Wiley: New York, 1980; p 26.

(25) The mass normally used to follow isobutylene oxide,  $m/q = 42$ , would be inappropriate for this experiment since  $42 + 2 = 44$  and  $\text{CO}_2$  would interfere with this experiment. The parent of isobutylene oxide,  $m/q = 72$ , is a small mass fragment and thus is responsible for the poor signal-to-noise observed in Figure 6b.

(26) Brainard, R. L.; Miller, T. M.; Whitesides, G. M. *Organometallics* **1986**, *5*, 1481–1490.

(27) Brainard, R. L.; Whitesides, G. M. *Organometallics* **1985**, *4*, 1550–1557.

(28) Foley, P.; DiCosimo, R.; Whitesides, G. M. *J. Am. Chem. Soc.* **1980**, *102*, 6713–6725.

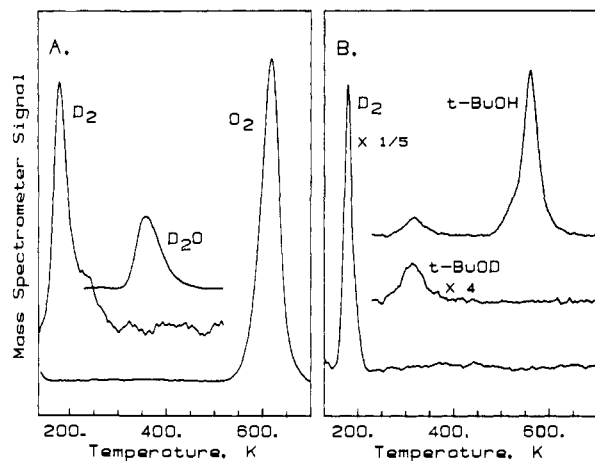


**Figure 8.** (A) TPRS spectra resulting from heating a Ag(110) surface covered with 0.08 ML  $D_{(a)}$  and 0.08 ML  $O_{(a)}$  at 8 K/s. (B) TPRS spectra resulting from heating a Ag(110) surface covered with 0.04 ML  $t\text{-BuO}_{(a)}$  and 0.1 ML  $D_{(a)}$  at 8 K/s. Spectra are corrected for mass spectrometer sensitivities.

molecular reactions have lower preexponential factors expressed in the same units<sup>33</sup> in the range of  $10^7$ – $10^{12}$   $s^{-1}$  for surface coverages near  $10^{-1}$  ML.<sup>29,34,35</sup> The low-temperature (oxygen-assisted) reaction observed here has a preexponential factor ( $A = 10^{9.4}$   $s^{-1}$ ) that is appropriate for a bimolecular reaction, although it is large enough to represent a unimolecular reaction that has a highly ordered transition state. Similarly, the reaction producing acetone ( $A = 10^8$   $s^{-1}$ ) may be bimolecular or unimolecular with a highly ordered transition state. The high-temperature reaction ( $A = 10^{6.4}$   $s^{-1}$ ) is probably a bimolecular process since the preexponential is too low to be accounted for by a unimolecular reaction with a highly ordered transition state. The preexponential factor expected for a unimolecular decomposition of  $t\text{-BuO}_{(a)}$  in which  $3^\circ$  of rotational freedom are lost in the transition state is estimated to be  $\log A = 11 \pm 1$  (see Appendix). It must be further noted that the coverages of  $t\text{-BuO}_{(a)}$  were approximately 0.2 and 0.1 ML, respectively, at the onset of the two channels, and the possible effect of steric interactions among the bulky *tert*-butoxy groups on the preexponential factors is difficult to assess. The fact that the frequency factor is *larger* in the low-temperature channel where the coverage of  $t\text{-BuO}_{(a)}$  is *higher* mitigates against an *increase* in the steric hindrance in the reaction at 510 K. Thus the lowering of the preexponential factor in the high-temperature channel does not appear to be due to steric hindrance.

**Recombination Reactions of Surface Hydrogen.** The isotopic labeling and the kinetic isotope effect experiments indicate that the rate-limiting steps for the reactions occurring at 440 and 510 K involve C–H(D) bond breaking, yet these processes do not produce dihydrogen ( $H_2$ ). Instead, hydrogen leaves the surface as water or *tert*-butyl alcohol. In order to address the question of whether the C–H bond breaking reactions involve surface-bound

hydrogen ( $H_{(a)}$ ) as a discrete reaction intermediate that reacts with  $t\text{-BuO}_{(a)}$  and  $O_{(a)}$  in preference to recombination to form  $H_2$ , or whether these reactions involve direct proton transfer to  $O_{(a)}$  or  $t\text{-BuO}_{(a)}$ , we prepared silver surfaces covered with both  $D_{(a)}$  and  $O_{(a)}$  or  $D_{(a)}$  and  $t\text{-BuO}_{(a)}$  and studied the recombination reactions of these adsorbates with TPRS.

An Ag(110) surface covered with 0.08 ML  $O_{(a)}$  and 0.08 ML  $D_{(a)}$  at 137 K was prepared by positioning the oxygen-covered surface 3 mm from a 1300 K platinum filament and dosing with 3 langmuirs of  $D_2$ . The TPRS spectrum (Figure 8A) resulting from this treatment shows large  $D_2$  and  $O_2$  peaks and a much smaller  $D_2O$  peak due to hydroxyl ( $OD_{(a)}$ ) recombination.<sup>17</sup> Integrated ratios for these peaks are 4.2:4.8:1.0, respectively. From these product ratios we can estimate the  $D_{(a)}$  reacts at least twice as fast with itself than it does with  $O_{(a)}$  to form  $OD_{(a)}$ .<sup>36</sup> This estimate should be considered the lower limit for this ratio of rates since deuterium atoms in the gas phase might react directly with  $O_{(a)}$  during their dose and form  $OD_{(a)}$ . The major conclusion from this experiment, however, is that the relative rates of  $D_{(a)} + D_{(a)}$  recombination vs  $D_{(a)} + O_{(a)}$  recombination may be comparable below 180 K (deuterium recombination temperature). Application of these results to the reactions occurring at 500 K, however, is difficult because the relative reaction rates may change considerably over this range of temperatures. However, the similarity in reaction rates makes it impossible to completely rule out mechanisms that involve transfers of hydrogen to the surface to form  $H_{(a)}$ , though we would expect to see  $H_2$  formation via recombination if  $H_{(a)}$  were formed.

An Ag(110) surface covered with ca. 0.04 ML  $t\text{-BuO}_{(a)}$  was prepared by dosing the Ag(110) surface at 200 K covered with 0.02 ML  $O_{(a)}$  with 0.22 langmuirs of *tert*-butyl alcohol followed by annealing to 345 K. Since the adsorbed oxygen does not form islands on this surface under our dosing conditions, there is no reason to expect islands of *tert*-butoxy species. A coverage of 0.1 ML  $D_{(a)}$  was added to this surface by positioning the crystal 3 mm from a platinum filament at 1300 K and exposing the filament to 4.7 langmuirs of  $D_2$ . A TPRS spectrum following this treatment (Figure 8B) showed that very little  $D_{(a)}$  reacted with  $t\text{-BuO}_{(a)}$  to form  $t\text{-BuOD}$ . From the relative yields of  $D_2$  and  $t\text{-BuOD}$  (260:1) and the initial coverages of  $D_{(a)}$  and  $t\text{-BuO}_{(a)}$ , we estimate that  $D_{(a)}$  reacts  $\sim 100$  times faster with itself than it does with  $t\text{-BuO}_{(a)}$ . Due to the magnitude of this ratio of rates at 180 K, we conclude that  $D_{(a)}$  probably also reacts faster with itself at 510 K despite the large difference in temperature. Thus, we suggest that  $H_{(a)}$  is not a reaction intermediate in the C–H bond breaking reaction occurring at 510 K, since if  $H_{(a)}$  were formed, it would produce a detectable amount of  $H_2$ . In further support of this argument, we note that the decomposition of primary and secondary alcohols on this surface at 300 K produce both  $H_2$  and the parent alcohols by mechanisms thought to involve  $H_{(a)}$ .<sup>1,2</sup> Thus, it appears that the recombination of  $H_{(a)}$  with  $RO_{(a)}$  is competitive with  $H_{(a)} + H_{(a)}$  recombination at 300 K, and the absence of  $H_2$  as a product in reactions of  $t\text{-BuO}_{(a)}$  indicates that  $H_{(a)}$  is probably not an intermediate in the high-temperature reactions. Instead, the C–H bond may be transferred directly to the oxygen in  $t\text{-BuO}_{(a)}$  via a bimolecular process, consistent with the low frequency factor observed in the high-temperature channel. The alternative explanation is that the steric bulk of the *tert*-butyl group in  $t\text{-BuO}_{(a)}$  severely hinders the diffusion of hydrogen atoms and impedes their recombination. If this were the case however, access to the oxygen atom to form *tert*-butyl alcohol should also be blocked, and hydrogen atom recombination would remain competitive. We conclude that steric hindrance of hydrogen migration is not important.

**Mechanism.** The reaction products, the isotope effects, and the isotopic labeling ( $t\text{-BuOD}$ ) experiments indicate that C–H bond breaking reactions are rate-limiting for the processes occurring at 440 and 510 K. Experiments in which oxygen and  $t\text{-BuO}_{(a)}$  coverages were varied indicate that the C–H bond breaking re-

(29) Somorjai, G. A. *Chemistry in Two Dimensions: Surfaces*; Cornell University Press: Ithaca, NY, 1981; pp 361–366.

(30) The preexponential for the decomposition of formate to  $CO_2$  and  $H_{(a)}$  on Ni(110) has been reported to be  $\log A = 1.5 \times 10^{15}$  and  $1.5 \times 10^{11}$   $s^{-1}$  as determined by TPRS experiments: Falconer, J. L.; Madix, R. J. *Surf. Sci.* **1974**, *46*, 473–504. Wachs, I.; Madix, R. J. *Surf. Sci.* **1977**, *65*, 287.

(31) Decomposition of  $DCO_{2(a)}$  and  $D_{(a)}$  gives  $\log A = 16$ : Barteau, M. A.; Bowker, M.; Madix, R. J. *Surf. Sci.* **1980**, *94*, 303–322.

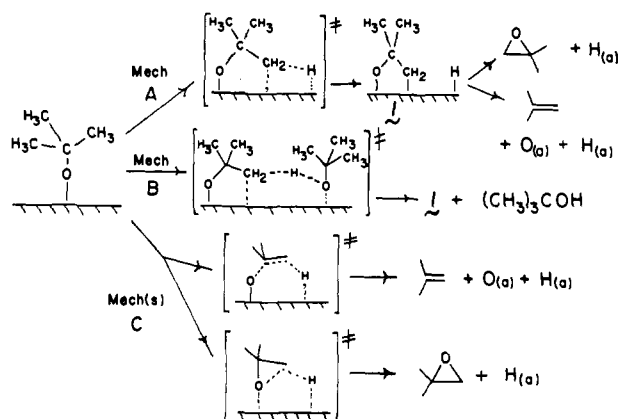
(32) Decomposition of  $CO_{3(a)}$  on Ag(110) to  $CO_2$  and  $OD_{(a)}$  gives  $\log A = 13$ : Bowker, M.; Barteau, M. A.; Madix, R. J. *Surf. Sci.* **1980**, *92*, 528–548.

(33) We express these preexponential factors in units appropriate for first-order reactions ( $s^{-1}$ ) since this simplifies comparison between reactions of differing molecularity and since it is not always possible to determine the molecularity of a reaction before examination of its preexponential.

(34) Bimolecular desorption of  $D_2$  from Cu(110) has a preexponential of  $10^{-7}$   $cm^2/s$  or, assuming a coverage of 0.1 ML  $D_{(a)}$ ,  $A = 10^7$   $s^{-1}$  [3]; Desorption of  $D_2$  from Ni(110)–(2  $\times$  1) C has a preexponential of  $3 \times 10^{-4}$   $cm^2/s$  or, at a coverage of  $6 \times 10^{14}$ ,  $A = 10^{11.3}$   $s^{-1}$ : Abbas, N.; Madix, R. J. *Surf. Sci.* **1977**, *62*, 739–750.

(35) Bimolecular recombination of  $2N_{(a)}$  to  $N_2$  in W(100) gives  $A = 10^{11.3}$   $s^{-1}$ : Clavenna, L. R.; Schmidt, L. D. *Surf. Sci.* **1970**, *22*, 365–391.

(36) Two  $OD_{(a)}$  form one  $D_2O$ . Hence, the reaction between two  $D_{(a)}$  is twice as fast as the reaction between  $D_{(a)}$  and  $O_{(a)}$  – not 4 times as fast.

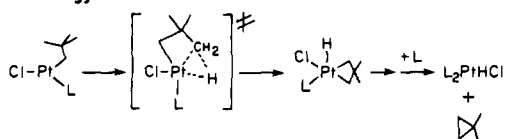
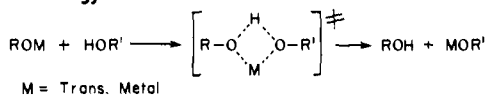
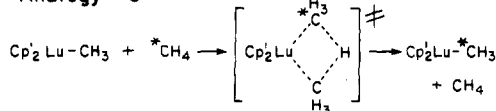
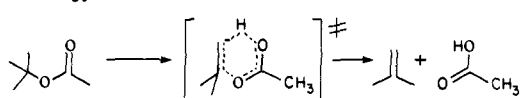
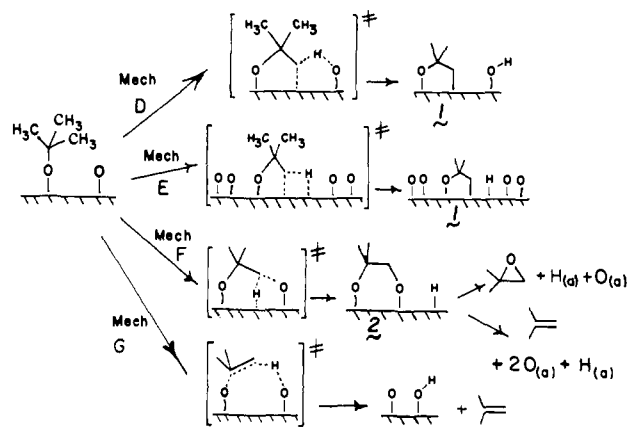
**Scheme III.** Possible Mechanisms for *t*-BuO<sub>(a)</sub> on Oxygen-Free Ag(110) Surfaces Occurring at 510 K

action occurring at 440 K is promoted by surface oxygen, since this reaction channel is favored by combining high coverages of O<sub>(a)</sub> and low coverages of *t*-BuO<sub>(a)</sub> (Figure 2). Conversely, the C-H bond breaking reaction occurring at 510 K is favored by low coverages of O<sub>(a)</sub> and high coverages of *t*-BuO<sub>(a)</sub>. Here surface oxygen (O<sub>(a)</sub>) is *not* directly involved in the initial C-H bond breaking reaction. The absence of H<sub>2</sub> as a reaction product, and the evidence that *t*-BuO<sub>(a)</sub> does not have an overwhelming capacity to preferentially scavenge H<sub>(a)</sub>, suggest that the proton-transfer reaction occurring at 510 K does not involve H<sub>(a)</sub> as an intermediate. Instead, the proton is probably transferred directly to *t*-BuO<sub>(a)</sub>. This implies an even greater stability of *t*-BuO<sub>(a)</sub> toward hydride transfer to the surface.

The dominant reactions are the formation of isobutylene oxide and isobutylene at 440 and 510 K. Since coadsorbed oxygen is not involved in the reaction at 510 K, at least initially, its mechanism will be considered first. Three plausible mechanisms for the decomposition of *t*-BuO<sub>(a)</sub> on the oxygen-free surface at 510 K are shown in Scheme III. Mechanism A involves the direct *rate-limiting* oxidative addition of silver atom(s) to a methyl C-H bond in *t*-BuO<sub>(a)</sub> yielding oxametallacycle **1** and H<sub>(a)</sub>. Oxametallacycle **1** rapidly decomposes via two competitive routes yielding isobutylene oxide or isobutylene and O<sub>(a)</sub>. Surface hydrogen (H<sub>(a)</sub>) then reacts with *t*-BuO<sub>(a)</sub> or O<sub>(a)</sub> yielding *t*-BuOH or H<sub>2</sub>O. Intramolecular C-H activation is well-known in the organometallic literature and is generally accepted to occur by mechanisms similar to mechanism A.<sup>26,28</sup> For example, a neopentyl-platinum complex reacts via intramolecular C-H activation yielding a metallacycle hydride (analogy A, Scheme IV).<sup>26</sup> Reductive elimination yields 1,1-dimethylcyclopropane. This last step is analogous to the reductive elimination of **1** from the surface to yield isobutylene oxide (Scheme II). This mechanism, however, is inconsistent with the absence of H<sub>2</sub> as a reaction product since H<sub>(a)</sub> reacts 100 times faster with itself than it does with *t*-BuO<sub>(a)</sub>. Further, the preexponential factor estimated for this reaction (see Appendix) is much higher ( $\log A = 11 \pm 1$ ) than observed experimentally ( $\log A = 6.4$ ).

A second possibility (mechanism B) is that two *t*-BuO<sub>(a)</sub>s react on the surface by proton transfer from a methyl carbon of one *t*-BuO<sub>(a)</sub> to the surface-bound oxygen of the other. This bimolecular mechanism is consistent with the low preexponential factor ( $\log A = 6.4$ ) and the decrease in peak temperature with increasing *t*-BuO<sub>(a)</sub> coverage. It is also consistent with the absence of hydrogen as a reaction product. This mechanism is similar to four-centered proton-transfer reactions common to the chemistry of metal alkoxides (analogy B)<sup>12</sup> and to the four-centered proton-transfer reaction proposed for methane activation by Cp<sub>2</sub>LuMe (analogy C).<sup>37</sup>

Alternatively, *t*-BuO<sub>(a)</sub> could decompose directly to products, without a metallacycle intermediate (mechanism C). The mechanistic pathway that forms isobutylene is similar to the

**Scheme IV.** Mechanistic Analogies**Analogy A****Analogy B****Analogy C****Analogy D****Scheme V.** Possible Mechanisms for Oxygen-Assisted Reaction Occurring at 440 K

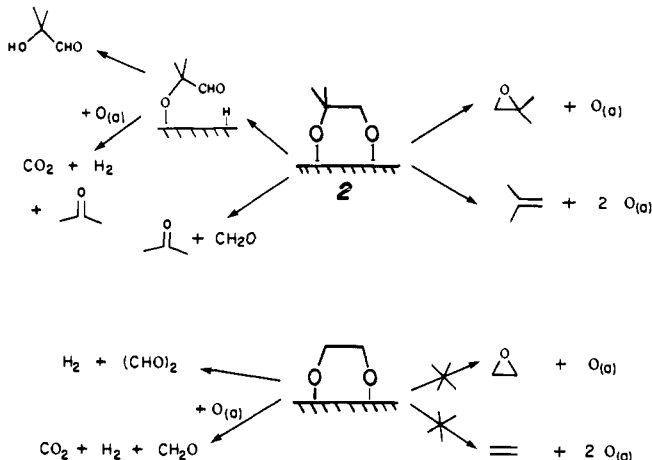
mechanism for the pyrolysis of esters (analogy D). *tert*-Butyl acetate decomposes via a six-membered cyclic transition state yielding acetic acid and isobutylene.<sup>38</sup> The major difficulty with this mechanism, however, is that it describes two distinct mechanistic pathways that produce either isobutylene oxide or isobutylene. Thus, this mechanism is not consistent with the results reported here, since the identical shapes of the isobutylene and isobutylene oxide TPRS peaks indicate that both products are produced by a single rate-limiting step. On the basis of the preceding arguments, we consider mechanism B as the most likely mechanism for the reaction occurring at 510 K.

The same mechanistic arguments used to explain the reaction at 510 K apply to the oxygen-assisted reaction at 440 K, except that hydrogen may be transferred either to silver or to adsorbed oxygen (mechanisms D and E in Scheme V). We have no basis with which to distinguish these two routes, since both hydroxyl disproportionation and the reaction of H<sub>(a)</sub> and O<sub>(a)</sub> to form water are rapid at this temperature. Attack of the C-H bond by O<sub>(a)</sub> at carbon yielding dioxametallacycle **2** and H<sub>(a)</sub> can be ruled out, however (Scheme V). It is conceivable that **2** could decompose yielding isobutylene oxide and isobutylene (Scheme VI). However, diglycolate (OCH<sub>2</sub>CH<sub>2</sub>O)<sub>(a)</sub> decomposes on Ag(110) surfaces to yield glyceraldehyde, formaldehyde, H<sub>2</sub>, and CO<sub>2</sub> (Scheme VI).

(37) Watson, P. L. *J. Am. Chem. Soc.* **1983**, *105*, 6491-6493.(38) Maccoll, A. In *The Chemistry of Alkenes*; Patai, S., Ed.; Interscience: New York, 1964; Chapter 3.

Table II. Cracking Fractions

compd	mass monitored								compd	mass monitored							
	42	56	59	58	18	2	44	28		42	56	59	58	18	2	44	28
isobutylene oxide	1.0	0.1	0.0	0.04	0.1	0.12	0.11	0.15	water	0.0	0.0	0.0	0.0	1.0	0.0	0.0	0.0
isobutylene	0.19	1.0	0.0	0.0	0.0	0.06	0.02	1.1	H <sub>2</sub>	0.0	0.0	0.0	0.0	0.0	1.0	0.0	0.0
tert-butyl alcohol	0.1	0.12	1.0	0.04	0.24	0.02	0.03		CO <sub>2</sub>	0.0	0.0	0.0	0.0	0.0	0.0	1.0	
acetone	0.67	0.0	0.0	1.0	0.0				CO	0.0	0.0	0.0	0.0	0.0	0.0	0.0	1.0

Scheme VI. Comparison of the Reactivity Patterns Expected for Metallacycle **2** with Those Observed for (OCH<sub>2</sub>CH<sub>2</sub>O)<sub>(a)</sub>

No ethylene oxide or ethylene is formed.<sup>39</sup> By analogy, metallacycle **2** would produce acetone, formaldehyde, H<sub>2</sub>, CO<sub>2</sub>, or HOC(CH<sub>3</sub>)<sub>2</sub>CHO, not isobutylene oxide and isobutylene. Second, <sup>18</sup>O is not incorporated into isobutylene oxide. One of the two pathways for metallacycle **2** to isobutylene oxide would lead to the incorporation of surface oxygen. Further, like mechanism C for the clean surface, mechanism G (Scheme V) can be ruled out since it requires two separate pathways for isobutylene and isobutylene oxide, and the identical shapes of the isobutylene and isobutylene oxide peaks indicate that both products are produced by a single rate-limiting step.

At this point we consider the implications of the reaction mechanism on the identity of the isobutene and isobutene oxide isomers discussed briefly in the Experimental Section. Though we have argued against the concerted rupture of the C–O and C–H bonds or the O–metal and C–H bonds in *t*-BuO<sub>(a)</sub>, we first consider the implications of such processes on product identity. If the transition state for butene formation involves cleavage of the C–O and C–H bonds in a concerted process, C–C double-bond formation would also occur, and isobutylene is clearly the product expected. It is conceivable that in the transition state for product formation from *t*-BuO<sub>(a)</sub> the carbon–hydrogen bond is completely or very nearly broken such that there exists transiently a radical, cation, or anion centered on the methylene carbon. The question is whether linear butenes or skeletally rearranged oxides can form from transition states such as these. It is well-known that methyl migrations do not occur in either radical or anionic intermediates, so that the hydrocarbon skeleton would not rearrange, and isobutylene would be the expected product.<sup>40–42</sup> On the other hand, an oxygen shift to the methylene carbon is possible, but such a rearrangement would be expected to yield either isobutylene oxide, or by hydride addition, isobutyraldehyde or isobutyl alcohol. The latter two products can be ruled out on the basis of the cracking patterns observed. The cation-like intermediate produced by

(39) Capote, A.; Madix, R. J., in progress.

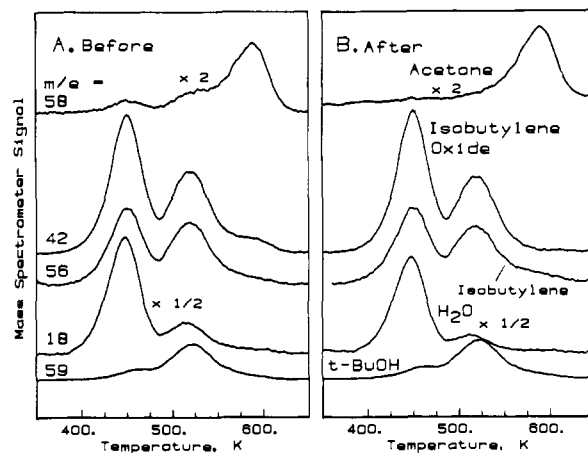
(40) Poutsma, M. L. Free-Radical Chlorination of Organic Molecules. In *Methods in Free-Radical Chemistry*; Huyser, S., Ed.; Marcel Dekker: New York, 1969; Vol. I.(41) Poutsma, M. L. Halogenation. In *Free Radicals*; Kochi, J. K., Ed.; John Wiley & Sons: New York, 1973; Vol. II.(42) DeMayo, P. *Rearrangements in Ground and Excited States*; Academic Press: New York, 1980; p 391.

Figure 9. (A) Raw TPRS spectrum before deconvolution. (B) Deconvoluted data.

hydride loss from *t*-BuO<sub>(a)</sub> could rearrange to give adsorbed 2-butoxide by a methyl migration to the methylene carbon and a concomitant shift of the positive charge to the carbon bound to the oxygen. This intermediate would be expected yield 2-butanone as an oxidized product, since only a simple electron rearrangement is required for the conversion and desorption. 2-Butanone was excluded on the basis of its cracking pattern, however. Other products such as tetrahydrofuran are rejected due to the rearrangements required for their formation, which are favored for neither cationic, radical, or anionic transition states. Similar arguments can be applied to further reaction of oxametallacycle **1** that involves cleavage of either the C–metal or O–metal bonds to form intermediates, leading to the conclusion that isobutylene and isobutylene oxide are indeed the product species.

The reactivity of *t*-BuO<sub>(a)</sub> differs appreciably from other alkoxides. Methoxide<sup>1</sup> and ethoxide<sup>2</sup> react on Ag(110) surfaces at 275–300 K by processes that involve breaking the C–H bond  $\alpha$  to oxygen at 275–300 K. These reactions occur at temperatures that are 210–235 K lower than the processes that break the methyl C–H bonds in *t*-BuO<sub>(a)</sub> in the absence of excess O<sub>(a)</sub>. We attribute this difference in reactivity to the difference between activated and unactivated C–H bonds. The activated  $\alpha$ -CH bonds in methanol, ethanol, and isopropyl alcohol (94, 93, and 91 kcal/mol, respectively) are weaker than that of a typical unactivated C–H bond (98 kcal/mol) such as that found in *tert*-butyl alcohol.<sup>43</sup> Another significant difference is that the primary and secondary alkoxides decompose by reaction pathways that involve H<sub>(a)</sub> as a reaction intermediate and thus produce H<sub>2</sub>. No H<sub>2</sub> is produced during the decomposition of *t*-BuO<sub>(a)</sub>. In addition, the presence of excess O<sub>(a)</sub> does not produce additional low-temperature pathways for the decomposition of the primary and secondary alkoxides.

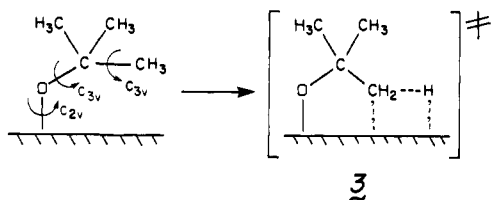
Precedent for oxygen-assisted C–H bond activation on Ag(110) exists. Acetate (CH<sub>3</sub>CO<sub>2(a)</sub>) reacts on Ag(110) by two processes involving C–H bond breaking.<sup>22</sup> Reaction occurs with an oxygen-covered surface much more readily than with the clean surface via methyl C–H bond activation by O<sub>(a)</sub>. The barrier to the oxygen-assisted decomposition pathway of acetate is 11 kcal/mol lower than the decomposition pathway in the absence of coadsorbed oxygen. Similarly, formate (HCO<sub>2(a)</sub>) is destabilized by the presence of surface oxygen, but by a lesser amount.<sup>21</sup>

(43) Benson, S. W. *Thermochemical Kinetics*; Wiley: New York, 1976.

Table III. Normalized Correction Factors

compd	mass fragment	correction factor
<i>tert</i> -butyl alcohol	59	0.57
isobutylene oxide	42	1.15
isobutylene	56	1.54
acetone	58	2.12
water	18	1.0
CO <sub>2</sub>	44	1.2
hydrogen	2	1.0
oxygen	32	1.26

Scheme VII. Formation of Cyclic Transition State 3



### Conclusion

*tert*-Butyl alcohol-*d*<sub>1</sub> reacts with O/Ag(100) below 200 K by breaking the O–D bond to form *t*-BuO<sub>(a)</sub> and D<sub>2</sub>O (eq 6).



*t*-BuO<sub>(a)</sub> reacts with oxygen-covered surfaces at 440 and 510 K to yield isobutylene oxide, isobutylene, water, and CO<sub>2</sub>. The mechanism for this process involves conversion of *t*-BuO<sub>(a)</sub> via rate-limiting C–H activation to an oxametallacycle that reacts rapidly via competing pathways to form the two products. The difference between the mechanisms on the clean and oxygen-covered surfaces lies in the precise role of oxygen in the C–H bond breaking process.

**Acknowledgment.** We gratefully acknowledge the donors of the Petroleum Research Fund, administered by the American Chemical Society, for the support of one of us (R.L.B.) during this research work. Partial support of the National Science Foundation (Grant NSF CBT 8701342) is also gratefully acknowledged.

### Appendix

**Decomposition of TPRS Data.** The raw TPRS data (Figure 9A) were deconvoluted by using a computer program<sup>15</sup> and the matrix shown in Table II, producing Figure 9B. This procedure was used so that the thermal desorption of a single compound could be followed without interference by the cracking fractions of other compounds. Figure 9 shows how contributions of isobutylene oxide and *tert*-butyl alcohol to *m/q* = 58 (acetone) complicate the TPRS spectrum of acetone.

**Correction Factors.** In order to quantify the TPRS desorption peaks, it was necessary to correct for differences in ionization efficiencies, mass spectrometer gain, mass fraction transmission, and the cracking of the parent molecule. For the most part, we followed the procedure described previously for determining correction factors,<sup>44,45</sup> except for the determination of ionization efficiencies. Ionization efficiencies were determined relative to water by an empirical method based on the total number of electrons.

The correlation for total ionization efficiency relative to CO<sup>45</sup> is a reasonable approximation for noble gases and for single metal atoms, but gives a very poor approximation for hydrocarbons and alkyl chlorides. A better approximation for the ionization efficiency relative to water for these molecules is given by an empirical correlation determined by George:<sup>46</sup>

$$I_x = 1.63 (\text{no. of electrons}/10) - 0.63 \quad (7)$$

The correction factors used in this study are listed in Table III.

**Thermal Effects on Cracking Patterns.** The initial thermal energy of a molecule entering a mass spectrometer can have a substantial effect on its ionization efficiency, appearance potentials, and cracking patterns, particularly at low ionization energies (~15 eV).<sup>47</sup> Although we used a moderately high ionization voltage (70 eV), we wished to rule out the possibility that a large change in the mass spectral fragmentation pattern of isobutylene (*m/q* = 56) with temperature could result in a disproportionate increase in the mass used to follow isobutylene oxide (*m/q* = 42), thus causing us to erroneously conclude that isobutylene oxide is a product. This specific question arises because of the nearly identical peak shapes of the isobutylene oxide and isobutylene products and because the temperature at which the reference spectra for the pure compounds were determined (190 and 300 K) differs from the temperature at which the reactions occur (440 and 510 K). We rule out such a qualitative error by comparison of the results reported here to the reaction of *tert*-butyl alcohol with the preoxidized Cu(110) surface,<sup>48</sup> which has been studied with the same mass spectrometer. This reaction involves the decomposition of *t*-BuO<sub>(a)</sub> at 500 K and produces isobutylene and (according to the same procedure) *no* isobutylene oxide. Thus, the *m/q* = 42 signal used to represent isobutylene oxide in this work cannot simply represent a change in the fragmentation pattern of isobutylene with temperature.

**Estimate of Preexponential for First-Order Decomposition of *t*-BuO<sub>(a)</sub> via a Highly Ordered Transition State.** We estimated the difference in entropy between *t*-BuO<sub>(a)</sub> and cyclic transition state 3 (Scheme VII) using procedures described by Benson.<sup>43</sup> We assumed that *t*-BuO<sub>(a)</sub> was completely free to rotate about its surface–O, O–C, and (CH<sub>3</sub>)–C bonds and that transition state 3 only had free rotation about two (CH<sub>3</sub>)–C bonds. (If, in fact, the rotation about the bonds in *t*-BuO<sub>(a)</sub> were restricted, our estimate of log *A* would be low.) We also assumed that *t*-BuO<sub>(a)</sub> has C<sub>2v</sub> symmetry about the Ag–O bond.

We also assumed that the loss in rotational entropy per bond in the conversion of *t*-BuO<sub>(a)</sub> to the cyclic transition state 3 was equal to the loss in rotational entropy per bond in the conversion of *n*-pentane to cyclopentane (–3.6 eu/bond). The entropic contributions of the two unchanged methyl groups cancel out.

$$S_{\text{rot}} = (5 \text{ bonds} - 2 \text{ bonds})(-3.6 \text{ eu/bond}) = -10.8 \text{ eu} \quad (8)$$

The correction for the symmetry of 3 and *t*-BuO<sub>(a)</sub> (Ag–O, C<sub>2v</sub>; O–C, C<sub>3v</sub>; Me–C, C<sub>3v</sub>) was calculated. Again the unchanged methyl groups cancel out.

$$\sigma = 2 \cdot 3^4 / 3^2 = 18 \quad (9)$$

$$S_{\text{sym}} = R \ln \sigma = 5.7 \text{ eu} \quad (10)$$

Thus, Δ*S*<sup>‡</sup> and *A* can be estimated:

$$S_{\text{tot}} = S_{\text{rot}} + S_{\text{sym}} \approx \Delta S^{\ddagger} = -10.8 + 5.7 = -5.1 \text{ eu} \quad (11)$$

$$A = 10^{13} \exp(\Delta S^{\ddagger} / R) = 10^{11.9} \text{ s}^{-1} \quad (12)$$

If the Ag–O bond is assumed to be asymmetric, and the ring bonds in 3 are assumed to be even more constrained (such as in cyclopropane: –4.9 eu/bond), then the preexponential is even smaller.

$$\Delta S^{\ddagger} = (3 \text{ bonds})(-4.9 \text{ eu/bond}) + R \ln 9 = -10.3 \text{ eu} \quad (13)$$

$$A = 10^{10.7} \quad (14)$$

Thus, according to this calculation, log *A* = 10.7 is the lower limit for the unimolecular decomposition of *t*-BuO<sub>(a)</sub>.

In a completely separate calculation, we assessed the entropy associated with the loss of rotational freedom of the same three bonds using a ridged rotor treatment.<sup>43</sup> This calculation involves

(46) George, S., work in progress.

(44) Ko, E. I.; Benziger, J. B.; Madix, R. J. *J. Catal.* **1980**, *62*, 264–274.  
 (45) UTI 100C Operating Manual. Uthe Technology, International, Sunnyvale, CA, 1975.

(47) Amorebieta, U. T.; Colussi, A. J. *Chem. Phys. Lett.* **1982**, *89*, 193–196.

(48) Brainard, R. L.; Madix, R. J. *Surf. Sci.*, in press.

many more assumptions than the first (e.g., rotational barriers in the starting species and frequencies of the vibrational modes in **3**), is rather long and involved, and is not reported in detail here. This second calculation is in general agreement with the first and gives  $\log A = 10$ .

Thus, according to both calculations, the preexponential for the reaction outlined in Scheme VI is approximately  $\log A = 11$

$\pm 1$ . Since it is much larger than the experimental value ( $\log A = 6.4$ ) for the high-temperature reaction, we conclude that it is unlikely that this reaction occurs by the unimolecular mechanism A (Scheme III).

**Registry No.** Ag(110), 7440-22-4; *tert*-butyl alcohol, 75-65-0; isobutylene oxide, 558-30-5; deuterium, 7782-39-0.

## Gas-Phase Acidities of Organosilanes and Electron Affinities of Organosilyl Radicals

Donna M. Wetzel, Karen E. Salomon, Susan Berger, and John I. Brauman\*

Contribution from the Department of Chemistry, Stanford University, Stanford, California 94305-5080. Received May 20, 1988

**Abstract:** We have measured the equilibrium gas-phase acidities for a series of alkyl- and aryl-substituted organosilanes, and the cross sections for electron photodetachment of the corresponding conjugate bases, using ion cyclotron resonance spectrometry. Gas-phase acidities for the conjugate acids of these compounds are  $\Delta H^\circ_{\text{acid}}(\text{SiH}_4) = 372.8 \pm 2$  kcal/mol,  $\Delta H^\circ_{\text{acid}}(\text{C}_6\text{H}_5\text{SiH}_3) = 370.7 \pm 2$  kcal/mol,  $\Delta H^\circ_{\text{acid}}(\text{C}_6\text{H}_5(\text{CH}_3)\text{SiH}_2) = 374.2 \pm 2$  kcal/mol,  $\Delta H^\circ_{\text{acid}}(\text{CH}_3\text{SiH}_3) = 378.3 \pm 2$  kcal/mol, and  $\Delta H^\circ_{\text{acid}}((\text{CH}_3)_3\text{SiH}) \geq 382.8 \pm 2$  kcal/mol. The electron affinities are  $\text{EA}(\text{SiH}_3^*) = 32.4 \pm 0.6$  kcal/mol,  $\text{EA}(\text{C}_6\text{H}_5\text{SiH}_2^*) = 33.1 \pm 0.1$  kcal/mol,  $\text{EA}(\text{C}_6\text{H}_5(\text{CH}_3)\text{SiH}^*) = 30.7 \pm 0.9$  kcal/mol,  $\text{EA}(\text{CH}_3\text{SiH}_2^*) = 27.5 \pm 0.8$  kcal/mol, and  $\text{EA}((\text{CH}_3)_3\text{Si}^*) = 22.4 \pm 0.6$  kcal/mol. These values were used to determine the Si-H bond dissociation energies in the organosilicon hydrides:  $D^\circ[\text{SiH}_3\text{-H}] = 91.6 \pm 2$  kcal/mol,  $D^\circ[\text{C}_6\text{H}_5\text{SiH}_2\text{-H}] = 90.2 \pm 2$  kcal/mol,  $D^\circ[\text{C}_6\text{H}_5(\text{CH}_3)\text{SiH-H}] = 91.3 \pm 3$  kcal/mol,  $D^\circ[\text{CH}_3\text{SiH}_2\text{-H}] = 92.2 \pm 3$  kcal/mol, and  $D^\circ[(\text{CH}_3)_3\text{Si-H}] \geq 91.0 \pm 2$  kcal/mol. The electronic structure of the organosilicon compounds studied is discussed and compared with that in the corresponding carbon compounds.

Thermochemical properties are indispensable tools for understanding chemical reactivity and making predictions about intermediates, products, equilibria, and reaction mechanisms. It is surprising, therefore, that despite the prolific investigation and utilization of organosilicon chemistry in the past 20 years, thermochemical data for organosilicon compounds remain scarce. For example, the data base of ionic, gas-phase thermochemical measurements<sup>1</sup> which has grown impressively in recent years has only minimal coverage in other classes such as organometallics. Especially important, yet experimentally challenging, are thermochemical measurements involving reactive silicon intermediates<sup>2</sup> such as divalent silicon compounds, silyl radicals, cations, and anions. In this paper, we report our measurements of the gas-phase acidities of selected organosilanes and the electron affinities of the corresponding organosilyl radicals.

In addition to contributing thermochemical data, gas-phase investigations involving equilibrium basicities and electron photodetachment spectroscopy of silyl and substituted silyl anions can provide information about substituent effects, hybridization, and electronic structure. This information, well known for carbon

compounds, is largely unavailable for organosilicon anions and radicals. Additional motivation for our experiments was the possibility of detailed comparisons between the behavior of silicon and carbon in anions and radicals.

Recent gas-phase investigations have contributed significantly to the understanding of silicon compound reactivity. Of particular interest are the studies involving negative ion-molecule reactions of silicon compounds.<sup>3</sup> Many important features of nucleophilic substitution reactions have been identified, with concomitant discovery of novel methods for generating a wide variety of organic anions and demonstration of stable pentavalent silicon anions. These studies have revealed excellent correspondence between reactivity patterns of silicon compounds in gas and condensed phases. Thus, the information gained on the behavior of gas-phase organosilyl anions, radicals, and neutral hydrides may enable direct correlation to solution-phase organosilicon chemistry.

We have measured the equilibrium constants for proton-transfer reactions between organosilanes (alkyl- and aryl-substituted silanes) and alcohols (alkoxide ions), from which the organosilane acidities can be determined. Gas-phase equilibrium measurements have been reported<sup>4</sup> only for  $\text{SiH}_4$ . Very recently, Damrauer, Kass, and DePuy<sup>5</sup> have reported gas-phase organosilane acidities, obtained from bracketing experiments performed in a flowing afterglow apparatus. The elegant design of the bracketing experiments allowed determination of both Si-H and C-H acidities. Our equilibrium results are generally in good agreement.

We have also measured the electron photodetachment cross sections for the corresponding organosilyl anions (conjugate bases). The only reported detachment data on organosilyl anions are

(1) Compilations include: (a) Bartmess, J. E.; McIver, R. T., Jr. In *Gas Phase Ion Chemistry*; Bowers, M. T., Ed.; Academic: New York, 1979; Vol. 2. (b) Drzagic, P. S.; Marks J.; Brauman, J. I. In *Gas Phase Ion Chemistry*; Bowers, M. T., Ed.; Academic: Orlando, FL, 1984; Vol. 3. (c) Kebarle, P.; Chowdhury, S. *Chem. Rev.* **1987**, *87*, 513.

(2) General reviews of some silicon reaction intermediates: (a) Raabe, G.; Michl, J. *Chem. Rev.*, **1985**, *85*, 419. (b) Bertrand, G.; Trinquier, G.; Mazerolles, P. In *Organometallic Chemistry Reviews*; Seyferth, D., Davies, A. G., Fischer, E. O., Normant, J. F., Reutov, O. A., Eds. *J. Organomet. Library*, 12; Elsevier Scientific Publishing Co.: New York, 1981. (c) Wiberg, N. *J. Organomet. Chem.* **1984**, *273*, 141. (d) Gusel'nikov, L. E.; Nametkin, N. S. *Chem. Rev.* **1979**, *79*, 529. (e) Gaspar, P. P. In *Reaction Intermediates*; Plenum Press: New York, 1980, 1981, and 1985. (f) West, R. *Pure Appl. Chem.* **1984**, *56*, 163. (g) Brook, A. G.; Baines, K. M. *Adv. Organomet. Chem.* **1986**, *25*, 1. (h) West, R. *Angew. Chem., Int. Ed. Engl.* **1987**, *26*, 1201. (i) Gaspar, P. P.; Holten, D.; Konieczny, S.; Corey, J. Y. *Acc. Chem. Res.* **1987**, *20*, 329.

(3) DePuy, C. H.; Damrauer, R.; Bowie, J. H.; Sheldon, J. C. *Acc. Chem. Res.* **1987**, *20*, 127.

(4) Bartmess, J. E.; Scott, J. A.; McIver, R. T., Jr. *J. Am. Chem. Soc.* **1979**, *101*, 6047.

(5) Damrauer, R.; Kass, S. R.; DePuy, C. H. *Organometallics* **1988**, *7*, 637.